

2021

Measurement and Theory of Gas-Phase Ion Mobility Shifts Resulting from Isotopomer Mass Distribution Changes

Christopher P. Harrilal

Viraj D. Gandhi

Gabe Nagy

Xi Chen

Michael G. Buchanan

See next page for additional authors

Follow this and additional works at: https://digitalcommons.georgefox.edu/bio_fac

 Part of the [Biology Commons](#)

Authors

Christopher P. Harrilal, Viraj D. Gandhi, Gabe Nagy, Xi Chen, Michael G. Buchanan, Roza Wojcik, Christopher R. Conant, Micah T. Donor, Yehia M. Ibrahim, Sandilya V. B. Garimella, Richard D. Smith, and Carlos Larriba-Andaluz

Measurement and Theory of Gas-Phase Ion Mobility Shifts Resulting from Isotopomer Mass Distribution Changes

Christopher P. Harrilal,

Biological Sciences Division, Pacific Northwest National Laboratory, Richland, Washington 99354,
United States

Viraj D. Gandhi,

Department of Mechanical Engineering, Purdue University, West Lafayette, Indiana 47907, United
States; Department of Mechanical and Energy Engineering, IUPUI, Indianapolis, Indiana 46202,
United States

Gabe Nagy,

Chemistry Department, University of Utah, Salt Lake City, Utah 84112, United States

Xi Chen,

Department of Mechanical Engineering, Purdue University, West Lafayette, Indiana 47907, United
States; Department of Mechanical and Energy Engineering, IUPUI, Indianapolis, Indiana 46202,
United States

Michael G. Buchanan,

Department of Mechanical and Energy Engineering, IUPUI, Indianapolis, Indiana 46202, United
States

Roza Wojcik,

Biological Sciences Division, Pacific Northwest National Laboratory, Richland, Washington 99354,
United States

Christopher R. Conant,

Biological Sciences Division, Pacific Northwest National Laboratory, Richland, Washington 99354,
United States; Present Address:

Micah T. Donor,

Biological Sciences Division, Pacific Northwest National Laboratory, Richland, Washington 99354,
United States

Yehia M. Ibrahim,

Biological Sciences Division, Pacific Northwest National Laboratory, Richland, Washington 99354,
United States

Sandilya V. B. Garimella,

Biological Sciences Division, Pacific Northwest National Laboratory, Richland, Washington 99354, United States

Richard D. Smith,

Biological Sciences Division, Pacific Northwest National Laboratory, Richland, Washington 99354, United States

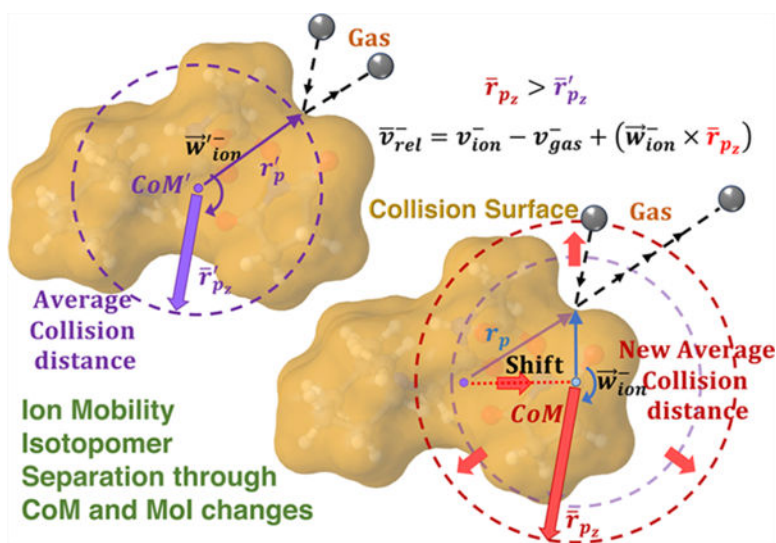
Carlos Larriba-Andaluz

Department of Mechanical and Energy Engineering, IUPUI, Indianapolis, Indiana 46202, United States

Abstract

The unanticipated discovery of recent ultra-high-resolution ion mobility spectrometry (IMS) measurements revealing that isotopomers—compounds that differ only in the isotopic substitution sites—can be separated has raised questions as to the physical basis for their separation. A study comparing IMS separations for two isotopomer sets in conjunction with theory and simulations accounting for ion rotational effects provides the first-ever prediction of rotation-mediated shifts. The simulations produce observable mobility shifts due to differences in gas–ion collision frequency and translational-to-rotational energy transfer. These differences can be attributed to distinct changes in the moment of inertia and center of mass between isotopomers. The simulations are in broad agreement with the observed experiments and consistent with relative mobility differences between isotopomers. These results provide a basis for refining IMS theory and a new foundation to obtain additional structural insights through IMS.

Graphical Abstract:



INTRODUCTION

Isotopomers are isotopic stereoisomers having the same number of nuclides but differing only in their locations. While mass spectrometry (MS) readily separates isotopologues,

isotopomers have identical mass and therefore cannot be distinguished by mass/charge (m/z) differences.^{1,2} As such, the recently reported observation of measurable shifts between isotopomers using ultra-high-resolution ion mobility spectrometry (IMS) separations in structures for lossless ion manipulations (SLIM)³ is unexpected. The only other reports^{4,5} of such isotopomer ion separation have involved differential or field asymmetric waveform IMS (FAIMS), where separations are dependent upon mobility differences in extremely high and low electric fields, making it difficult to understand their origin.

In all ion mobility experiments, ions move in a buffer gas due to the presence of an electric field, with mobilities dependent on the strength of the electric field. For example,^{6–8} the mobility of an ion (K), can be predicted using the two-temperature Mason–Schamp relationship, where μ is the reduced mass of the ion–neutral molecule pair, k_b is the Boltzmann constant, ze is the charge of the ion, α_c is a higher-order correction, T_{eff} is the effective ion temperature, N is the gas number density, and $\Omega(T_{\text{eff}})$ is the ion-neutral momentum transfer collision cross section (CCS)⁸

$$K = \frac{3}{16} \sqrt{\frac{2\pi}{\mu k_b T_{\text{eff}}}} \frac{ze(1 + \alpha_c)}{N\Omega(T_{\text{eff}})} \quad (1)$$

Based on eq 1 it has been broadly assumed that isotopologues should separate due to their reduced mass differences given sufficiently high IMS resolving power R_p .⁹ As anticipated, such separations have been observed in low^{3,10,11} electric fields in addition to those observed in the high field regime.^{10,12–14} Similarly, given eq 1, it has been assumed that mobility differences for isotopomers would be far too small or completely indistinguishable as their CCS would be indistinguishable from a theoretical perspective.⁴ However, the recently observed IMS isotopomer mobility shifts obtained from ultra-high-resolution SLIM IMS³ leads to the hypothesis that internal degrees of freedom, vibrational and rotational, must be a key element for such separation. Generally, such effects are largely ignored in most, if not all, CCS or mobility calculations.^{15,16} A theoretical possible alternative for incorporating the internal degrees of freedom for polyatomic systems would be the Wang–Uhlenbeck–de Boer equation (WUB).¹⁷ However, its use is not sufficiently extended for use in such complex systems, and one must resort to numerical schemes to account for internal degrees of freedom.

When looking to isolate the effect of vibrational degrees of freedom—leaving rotation aside—any difference in the WUB CCS should arise from the different vibrational energy levels manifested due to the distinct placement of the heavy labels. However, this CCS change is expected to be overall very similar, or indistinguishable, between isotopomers as all would have the same number of additional heavy labels, albeit at different positions. While not fully discarding such a vibrational effect, these considerations have led us to explore whether the observed experimental shifts arise mainly from ion rotational effects due to differences in the ion center of mass (CoM) and moment of inertia (MoI).

Here, we report on isotopomer IMS separations for two sets of isotopomers in combination with new theoretical and computational approaches. Computationally, we adopt a Monte Carlo simulation of the ion in a bath gas, explicitly accounting for ion rotational effects.

The simulations are consistent with the relative mobility differences observed between isotopomers, broadly confirming the measurements. This finding suggests a refinement of the current approach for numerical calculations that explicitly accounts for rotational degrees of freedom. A deeper understanding of the isotopomer ion separations and the dependence of their mobilities on the ion's CoM and MoI has fundamental and practical implications to analytical science and related applications.

EXPERIMENTAL SECTION

The long path length (13.5 m) multi-pass traveling wave IMS separations platform based upon SLIM coupled to mass spectrometry (i.e., SLIM IMS-MS) has been described in detail elsewhere.¹⁸ The SLIM IMS-MS experimental conditions used for iodoTMT isotopomers, described previously,³ were also used here for the TMT isotopomers (-126 , $127N$, $128N$, $129N$, $130N$, and 131 isotopomers from the TMT-10 plex series; Thermo Fisher Scientific, Waltham, MA). All six highest and the lowest mobility isotopomer ions are used to establish the mobility scale, with the remaining intermediate isotopomers assumed to be scaled linearly over the small mobility range. To simulate the effects of ion rotation on gas phase ion mobilities, Ion Mobility Software 2.0 (IMoS 2) has isotopomers for each set were prepared and run as mixtures (circumventing any potential issues associated with measuring their mobilities individually, e.g., density, temperature, and electric field variations being the same for all) of $10\ \mu\text{M}$ each in 50/50 water/methanol with 0.5% acetic acid (v/v) for ion generation using electrospray ionization (ESI) in the positive ion mode. Ions were accumulated in the SLIM prior to IMS separation, as previously described.³ SLIM IMS separations utilized 1.5 Torr nitrogen as the buffer gas and Traveling wave (TW) speeds of 300 m/s at 27 V amplitude (0-peak) and 400 m/s at 35 V (0-peak) for the separations of TMT and iodoTMT isotopomer ions, respectively. To determine the been employed as an extension of IMoS.^{16,20} IMoS 2 places a density functional theory (DFT)-optimized ionic structure [see Supporting Information (SI) for conformer generation and structures] in a neutral gas bath (NVT ensemble with periodic boundaries), as indicated in Figure 1a. The ion is treated as a rigid body that is subjected to an electric field E . As such, the rigid body accelerates, can rotate, and may be subjected to torque if a dipole-electric field interaction is present. As the ion accelerates, it collides with the gas, slowing its advance. The resulting ion velocity as a function of time may be extracted, as shown in Figure 1c, and the respective velocity distributions are shown in Figure 1b,d. Eventually, the arrival time distributions (ATD) for the mixtures of ions, on average, reach a “terminal” drift velocity v_d in the isotopomer ions (m/z 345 for $[\text{TMT} + \text{H}]^+$ and m/z 458 for $[\text{iodoTMT} + \text{H}]^+$), the ions were fragmented post-SLIM IMS separation to yield six distinctive nonisobaric fragment ions (Figures S1 and S2, extending from m/z 126 to 131), allowing their identification using an Agilent time-of-flight MS. All data were processed in the unified ion mobility format (.UIMF) and visualized in our homebuilt viewing software (URL: <https://github.com/PNNL-Comp-Mass-Spec/UIMFViewer>). The summation of large numbers of individual IMS separations was corrected for any ATD changes due to, e.g., small pressure, temperature, or electric field fluctuations between the individual IMS separations.¹⁹ In this, the ATD for all detected isotopomers from each separation are slightly shifted, resulting in a net improvement in the resolving power compared to the unaligned separations (see

Figure S3 for comparisons). As noted previously,³ the observed relative IMS shifts were not significantly dependent upon the conditions selected (including any possible field heating), which can be attributed to the expectation that all isotopomers would be impacted identically by any such changes. All experiments were performed in triplicate, and the error bars shown represent ± 1 standard deviation σ . A 3 ms moving average smoothing was used for the overlaid ATD for the isotopomer IMS shifts. Mobility shifts between isotopomers are given in a linear, normalized, relative scale in Table 1. The arrival time of the direction of the field (x), while their velocity averages to zero in the other two directions. The mobility can then be calculated through the simple relation $v_d = KE$. In this work, where the objective is to study the effect of ion rotation, a constant electric field was employed, and no dipole moment or attractive potential interactions were considered. Note that high field effects, except those pertaining to vibrations, will be taken into account. These include a different effective temperature for the ion (field heating) and a different exchange of energies between rotation and translation.

Upon a gas-ion collision, both linear and angular momentum are exchanged, and energy is conserved. The post-collision linear and angular velocities of the ion, \vec{v}_{ion}^+ , \vec{w}_{ion}^+ are given by

$$\vec{v}_{\text{ion}}^+ = \vec{v}_{\text{ion}}^- + \frac{\widehat{j\vec{n}}}{m_{\text{ion}}} \quad (2a)$$

$$\vec{w}_{\text{ion}}^+ = \vec{w}_{\text{ion}}^- + I_{\text{ion}}^{-1}(\vec{r}_p \times \widehat{j\vec{n}}) \quad (2b)$$

where \vec{v}_{ion}^- and \vec{w}_{ion}^- are the linear and angular velocities of the ion before the collision, I_{ion} is the MoI of the ion \vec{r}_p is the distance from the point of collision to the CoM of the ion, $\widehat{j\vec{n}}$ is the impulse vector in the normal direction $\widehat{\vec{n}}$ outward of the collision point, and $\vec{r}_p \times \widehat{j\vec{n}}$ is the impulsive torque, where \times represents a cross product. The impulse vector may be written as

$$\widehat{j\vec{n}} = - \frac{2v_{\text{rel}_n}^- \widehat{\vec{n}}}{\frac{1}{m_{\text{ion}}} + \frac{1}{m_{\text{gas}}} + \widehat{\vec{n}} \cdot \left(I_{\text{ion}}^{-1}(\vec{r}_p \times \widehat{\vec{n}}) \times \vec{r}_p \right)} \quad (3)$$

with the normal component of the relative velocity, $v_{\text{rel}_n}^-$, given by

$$v_{\text{rel}_n}^- = \widehat{\vec{n}} \cdot (\vec{v}_p^- - \vec{v}_{\text{gas}}^-) \quad (4)$$

$$\vec{v}_p^- = \vec{v}_{\text{ion}}^- + \vec{w}_{\text{ion}}^- \times \vec{r}_p \quad (5)$$

where \vec{v}_p^- and \vec{v}_{gas}^- are the ion's velocity at the point of contact and the gas molecule's velocity prior to the impact. Based upon eqs 2a, 2b–5, if a shift is numerically observed

between two different isotopomers, it can be ascribed to only two possible effects, both of which are relatively linked to the MoI and CoM (through \vec{r}_p). The first effect, which is perhaps quite intuitive, may be extracted from eq 2b and deals with the fact that different angular velocities lead to different collision frequencies with the neutral gas. The second effect is embedded into eqs 2a, 2b–5, where the relative change in motion of the ions after a collision is affected by the MoI and CoM through its effect on the impulse ($\widehat{j\vec{n}}$) and the impulsive torque ($\vec{r}_p \times \widehat{j\vec{n}}$); specifically, how much the ion is slowed down (or sped up), \vec{v}_{ion}^+ , per collision, depends on the partitioning of the collisional energy between the rotational or translational degrees of freedom. However, the values of MoI and CoM are coupled and are structure-dependent, so the contribution of each effect is difficult to separate for a complex ion and hence a key challenge in this analysis.

The shift in mobilities between isotopomers is expected to be a small perturbation (a fraction of a percent) due to the relatively small contribution of rotation. Thus, a sizeable number of gas collisions are necessary to provide sufficient precision in the calculations. The IMoS 2.0 algorithm was parallelized using 432 cores and run for 150 μ s on each core, totaling ~65 ms of total drift time, yielding approximately 1.2 billion collisions for each structure studied.

RESULTS AND DISCUSSION

Figure 2a,c shows the experimentally observed arrival times for the iodoTMT and TMT isotopomers, respectively. Within each mobiligram, the arrival time distributions can be separated into three distinct groupings. For iodoTMT (Figure 2a), the order is: –126/–127, followed by –128/–129 and then by –130/–131, with relatively minor shifts observed between the indicated pairs. For the TMT isotopomers (Figure 2c), the –126/–127/–128 isotopomers arrive in the first group, followed by –130/–129 and then by –131, with again only small differences within the subgroups. Clearly, isotopomers with heavy atom substitutions in similar locations have similar mobilities. For iodoTMT isotopomers, the first group (–126/–127) has heavy labels largely located along the backbone. In the second group (–128/–129), the heavy labels are split between the substituted piperidine ring and the backbone. While in the third group (–130/–131), the majority of the heavy labels are within the piperidine ring. For TMT isotopomers, the first and fastest group (–126/–127/–128) has the most heavy labels on the backbone and the second group (–130/–129) has heavy label locations split between the piperidine ring and backbone atoms, while the lowest mobility, –131, has all of the heavy label sites on the piperidine ring. Also, apparent for both isotopomer sets is a mobility decrease when heavy label sites are near the piperidine ring.

The relative numerical simulated arrival times for the iodoTMT and TMT isotopomers with respect to the 126 isotopomer (highest mobility) are shown in Figure 3. Error bars represent the standard error as σ/\sqrt{n} , with n being the number of computational cores (432). While the shifts, number of collisions, and overall error depend on the field employed and total time sampled, these raw results provide insight into the overall shift percentage and error from the simulations and indicate mobility shifts smaller than 0.3% (3000 ppm) with standard deviations corresponding to 100–200 ppm. For comparison, the simulated

results are scaled similarly to the experimental results and are given in Table 1. They show remarkable agreement with the experimental observations. A couple of deviations are worth mentioning here. While the order of TMT-129 and TMT-130 is switched, their experimental mobilities are extremely close (as seen in Figure 2). In terms of the simulations and the discussion below, the trend of isotopic distributions going toward the piperidine ring suggests that TMT-129 might arrive slightly faster but very close. As for iodoTMT-127, it appears outside of the margin of error, suggesting that there may be other effects at play that are not presently reconciled. Given the agreement, one can confidently confirm that the experimental shifts observed are real and that the major contribution to the shifts seems to be due to ion rotation. To arrive to this conclusion, alternative explanations were considered, such as internal vibrations, which are not taken into account as the simulations consider a single optimal DFT structure with a fixed MoI and CoM. Regarding the structure, the very slightly shortened bond lengths resulting from heavy atom substitutions are insufficient to alter geometries sufficiently to produce the observed IMS shifts. As an example, the ten lowest relative energy structures for unlabeled TMT (i.e., without any isotopic substitutions) and TMT-130 were nearly indistinguishable with regards to geometry. Furthermore, the relative energies between conformations for the isotopomers are nearly identical (see Tables S1 and S2). Also, there is no expectation that other factors, such as potential interaction considerations, would be significantly different between isotopomers since the interaction with the background gas is randomized in all directions and is not expected to have isotope-dependent effects (the added computational cost of potential interaction calculations also advocated for their omission in the present study). Differences in deformations upon impact collisions between isotopomers is expected to be negligible as the differences in translational-to-vibrational exchanges, due to the vibrational differences from isotopic changes, are expected to be insignificant at the low electric field used, as evidenced from observations and field calculations during these separations.³

Thus, discarding for the time being possible alternative reasons for the shifts, we now focus on the more subtle relationship between rotation and mobility. Changes to the MoI, whether through changes of the CoM or not, affect the angular velocity of the ion, impacting collision frequencies. At the same time, both MoI and CoM through \vec{r}_p affect the details of energy transfer between rotational and translational degrees of freedom during collisions (see eqs 2a, 2b–5, and 6 below), ultimately affecting the mobility. The convolution of these considerations as well as their sensitivity to details of the collisional interactions begs two key questions: can the experimentally observed mobility shifts be predicted by extended computational approaches that include ion rotational effects and how sensitive are these shifts to structural changes? While one cannot fully directly address the latter question here, addressing the former will provide the basis for its future consideration.

ISOTOPOMER CENTER OF MASS AND MOMENT OF INERTIA CHANGES

The comparison of the experimental shifts to changes in the CoM and MoI appears most pertinent. Equation 3 shows the dependence of $\left(\widehat{j\vec{n}}\right)$ on both \vec{r}_p (CoM-related change) and MoI. Ideally, to understand the role and magnitude these changes play in determining the mobility shift of an ion, a single parameter would be adjusted at a time. While it is

complicated for real isotopomers, since both are inherently coupled under most scenarios, it is possible to understand how changes in each of these parameters affect the mobility of an ion in a decoupled manner using simulations. Several results are shown in Figure 4 for strategically designed artificial isotopomer systems such that the mobility shifts can be characterized in a well-defined manner. These systems are created by placing the 5 Da isotopic substitution masses in any artificial location of choice. Mobility shifts are all referenced to a “base” molecule: a molecule that has the extra 5 Da from the isotopic substitutions placed at the CoM of the “zero” substitutions molecule. The base molecule will have the same CoM and MoI as the zero molecule. Moreover, given the parallel axis theorem, moving the 5 Da from the base molecule’s CoM to any other location must increase its MoI. Therefore, this base molecule will always be the isotopomer with the smallest MoI, and constitute a suitable reference (blue square Figure 4). In all cases, the additional mass does not affect the geometrical structure and does not interact with gas molecules, even when located outside of the molecule structure. Once simulations are completed, relative shifts in drift velocity (mobility) greater than 1 represent shifts to lower drift velocities (mobilities) with respect to the base molecule, and the opposite for values less than 1.

In the simplest case, one can look at the effects of increasing the MoI without changing the CoM. Accordingly, simulations used fifty 0.1 Da masses uniformly positioned on a sphere centered on the CoM of the zero/base molecule (hence not modifying \vec{r}_p). This was repeated for spheres of radii 4 and 8 Angstroms (Å). Table S3 provides average values of the MoI of real and artificial isotopomers as well as other values of interest. Figure 4 shows the relative mobility shifts for the MoI-only changes as a function of the average collisions per core (dark empty diamonds connected by a black line). The mobilities of these artificial isotopomers for iodoTMT and TMT decrease (i.e., display increased ATDs) relative to their respective base isotopomer while at the same time experiencing fewer collisions.

While it is simple to isolate the effect of a change of the MoI while keeping the CoM constant, it is not as straightforward to create an artificial isotopomer in which the CoM is altered while keeping the MoI the same. Rather, a series of artificial isotopomers were created by displacing the 5 Da mass from the CoM in different coordinate directions. The resulting effects of these shifts depend on the orientation of the DFT molecule, where the x-direction corresponds to the backbone (Figure S5, coordinates provided in Tables S4 and S5). In light of this, the extra 5 Da were placed at one single location 4 and 8 Å away from the base molecule’s CoM in the *x*, *y*, and *z* coordinates, and in both positive and negative directions. CoM shifts with respect to the base molecule correspond to 0.05814 Å for TMT and 0.0467 Å for iodoTMT for every 4 Å change. Figure 4 shows the relative mobility shifts corresponding to iodoTMT and TMT artificial mass shifts, where dashed lines are drawn connecting the shifts in a particular direction and orientation (labeled as *x*_{pos}, *x*_{neg}, etc.). A key observation is that the mobility shifts are quite different when placing 5 Da at different locations. For example, a change in the positive *x*-direction for iodoTMT isotopomers produces a shift toward lower mobility, while a change in the negative *x*-direction produces a shift toward higher mobility (blue dotted line Figure 4a). The opposite happens for TMT (blue dotted line in Figure 4b). For both iodoTMT and TMT, the changes in the *y*- and

z -directions are not as pronounced as in the x -direction, and overall, all changes seem to be somewhat symmetric with respect to the MoI-only change curve. It is noted that the shifts to lower mobilities are not necessarily accompanied by an increase in the collision frequency, as one might expect. These results might be puzzling at first since the base molecule, which theoretically has the smallest MoI (and therefore assumed to have the highest angular velocity and collision frequency), does not necessarily have the overall lowest mobility. In fact, its resulting mobility leans higher. This, while counterintuitive at first, can be rationalized from an energy perspective using a modified Wannier's formula.^{6,21} The overall energy balance of the ion for translational and rotational degrees of freedom is

$$\frac{1}{2}m_{\text{ion}}\left(v_{\text{d}}^2 + \overline{V^2}\right) + \frac{1}{2}\vec{\omega}^T \vec{I}_{\text{ion}} \vec{\omega} + E_{\text{diffE}} = E_{\text{elec}} + 3k_{\text{b}}T \quad (6)$$

where v_{d} is the drift velocity, $\overline{V^2}$ is the averaged squared molecular speed of the ion, and T is used to represent the transpose of the angular velocity. In this equation, the total electrical (E_{elec}) and thermal energies, $3 kT$ for 6 degrees of freedom, must equal the kinetic energy of the ion, $m_{\text{ion}}(v_{\text{d}}^2 + \overline{V^2})/2 = m_{\text{ion}}v_{\text{d}}^2/2 + 3k_{\text{b}}T/2$ the rotational energy, $\vec{\omega}^T \vec{I}_{\text{ion}} \vec{\omega}/2$, and the excess diffusion/randomization collisional energy due to the field, E_{diffE} , which corresponds to the diffusion component of the energy dissipated into the gas. In Wannier's formula, $E_{\text{diffE}} = m_{\text{gas}}v_{\text{d}}^2/2$; however, this would not be exact here, given that part of the impulsive torque would go into randomization as well.

The effect of this randomization simply results in a larger standard deviation over that of the expected thermal noise, $\sqrt{k_{\text{b}}T/m}$, as apparent in Figure 2c. Considering eq 6 by itself, one could suggest that a change in MoI could be compensated by a decrease in angular velocity alone.

However, the coupling of angular and linear momentum in eqs 2a, 2b–5 suggests that a change in the MoI/CoM would also affect the drift velocity (and hence the mobility) of the ion through the impulse and impulsive torque. Indeed, an increase of the MoI can be equilibrated by a combination of a decrease in angular velocity together with an increase/decrease in mobility. The mobility may therefore shift in any direction as predicted by simulations (Figure 4). How this effect occurs is quite convoluted and depends directly on the structure (see Section S3.2).

In the case of MoI-only changes where the CoM (\vec{r}_{p}) value is kept consistent relative to the base isotopomer, the results can be rationalized. Figure 4 (MoI-Only change curves) shows that as the MoI increases, the relative mobilities decrease while concomitantly experiencing fewer collisions relative to the base isotopomer. This might be surprising at first, as the decrease in angular velocity due to the increase in MoI (which can be extracted from simulations) may lead to the expectancy of an increase in mobility. Equations 2a, 2b, and 3, however, reveal that an increase in the MoI increases the overall impulse (from the $I_{\text{ion}}(\vec{r}_{\text{p}} \times \vec{\omega}) \times \vec{r}_{\text{p}}$ term in the denominator). The increase in collisional impulse leads to an overall reduction of the drift velocity as more energy is provided to the gas

per collision, slowing the advance. A reduction of the drift velocity also decreases the collision frequency. Comprehensively, the mobility shift must therefore be a competition between the decrease in angular velocity and the increase in collisional impulse. It seems from the MoI-only simulations that the effect of the reduction in the drift velocity due to the resulting changes in the impulse vector outweighs the effect of reducing the angular velocity. Thus, an increase in the MoI without a modification of the CoM leads to lower mobilities and collision frequencies. The effect, although visible, is small. For perspective, the relative mobilities from the simulations of the real isotopomers –126 to –131 for iodoTMT and TMT, referenced to the base isotopomer, are shown for comparison in Figure 4a,b. The largest MoI increases of the artificial MoI-only changed isotopomers for iodoTMT and TMT correspond to 4.6 and 7.8%, resulting in mobility shifts of 0.18 and 0.25%, respectively. The MoI changes for the real –131 isotopomer (largest MoI of both sets) for iodoTMT and TMT are 1.6 and 1.3% and correspond to relative mobility shifts of 0.29 and 0.18%, respectively. Thus, the real isotopomer mobility shifts are of similar magnitude to the artificial isotopomers but have much smaller increases in their MoI relative to the base isotopomer. It is clear then that the MoI-only changes are insufficient to explain the overall shifts for the real isotopomers. They also seem to only decrease mobility over the base molecule, which does not seem to explain all behaviors encountered as some of the isotopomers are seen to increase in mobility.

It should be made clear at this point that, given that there are three principal directions for the moment of inertia, isotopic shifts may affect the principal values differently. Given that the MoI change alone is insufficient to explain the shifts, the effect of varying \vec{r}_p must be just as important, if not more. The CoM changes of the real isotopomers relative to the base isotopomer are given in Figure S6. For example, the TMT-131 CoM change with respect to the base molecular ion is given by $(-0.041, -0.0015, 0.006)$ Å corresponding to a (x, y, z) variation. As the negative x -direction variation largely dominates, one would expect the TMT-131 isotopomer to shift toward lower mobilities with respect to the base molecule, as predicted in Figure 4. In fact, the observed change is quite close to the artificial isotopomer with a CoM of $(-0.05814, 0, 0)$ Å. Furthermore, one can also observe qualitative agreement between collision frequencies of real and artificial isotopomers. In the case of TMT-126 with a CoM change of $(0.0070, 0.0295, 0.0049)$ Å, one would expect its mobility shift to be between the y positive and x positive lines, which is what is observed from the artificial simulations. The collision frequency should also be lower than that for TMT-131. Analogous observations can be made for the other TMT and iodoTMT isotopomers, the latter having large positive x -direction CoM variations (Figure S6a). Thus, we can assume that a combination of artificial CoM changes may be used to predict shifts in mobility as long as the MoI change is somewhat similarly replicated. For example, a combination of artificial changes may lead to the same CoM as TMT-131, but given that the extra 5 Da of mass is bundled, it will not yield the same MoI. For the TMT and iodoTMT molecules, the differences between the MoI change of –131 and that of a CoM-equivalent change artificial isotopomer are minimal (i.e., $\langle I_{\text{artif}} \rangle / \langle I_{131} \rangle = 0.998$), so only small deviations are expected.

RELATIVE MOBILITY DEPENDENCE ON CHANGES IN ISOTOPOMER CENTER-OF-MASS (COM)

A final key question to address is why the mobility shifts become positive or negative depending on the shift of the CoM. Given that the mobility shift cannot be due solely to changes in the MoI and must be contingent on molecule geometry (it differs depending on the axis used to shift the CoM), it is safe to assume that the reason lies in how \vec{r}_p changes with the CoM.

Given that \vec{r}_p is the distance between the ion-neutral point-of-impact and the CoM, the farther away the point of impact is from the CoM, the higher the relative velocity ($\vec{w}_{ion} \times \vec{r}_p$) at that point, assuming no differences in \vec{w}_{ion} ; hence, the stronger the momentum exchange interaction will be upon collision, giving more energy to the gas and subsequently slowing the ion more per collision. For this reason, one can attempt to study how global changes in collision distance to the CoM affect mobility. To illustrate this point, one can use the 2D structure in Figure 5a,b, whose angular velocity is off-plane and where the sole difference between the two structures is the location of the CoM. One can calculate the locus of possible positions, where a collision might take place given by a dashed line surrounding the structure that adds the radii of the gas molecule. However, if one were to calculate the average distance to the collision surface, \bar{r}_{p_z} , for each CoM depicted in Figure 5, the results differ, as shown by the different sized circles. Assuming the same initial angular velocity for both structures, and if all collision points have the same probability of getting struck, there is an expectancy that the structure with the larger \bar{r}_{p_z} will presumably yield the smaller mobility. There is also the expectancy that a larger \bar{r}_{p_z} signifies a larger swept area farther from the CoM, which should increase the collision frequency.

This same concept may be extended to three-dimensional (3D) structures. The locus of collision points in this case corresponds to the Connolly (molecular) surface,²² A_{Co} , which is shown in Figure 6a for iodoTMT and Figure S7a for TMT. Assuming that all collision points on the surface are equally probable, one can average the collision distance with respect to an axis i that passes through the CoM

$$\bar{r}_{p_i} = \frac{1}{A_{Co}} \oint r_{p_i} dA_{Co} \quad (7)$$

The reason why the distance to an axis is used and not the absolute distance to the CoM is to distinguish the effect of rotation along different axes. Larger values of \bar{r}_{p_i} result in a larger fraction of the collision area farther away from the axis of rotation, and hence higher relative velocities, higher impulses, and possibly lower drift velocities. This can then be used to compare the \bar{r}_{p_i} values of artificial isotopomers to the base isotopomer. Provided that the artificial isotopomer CoM shifts are given with respect to an axis, one can use a second index to describe an artificial isotopomer shift in a particular direction. For example, for an isotopomer with a determined CoM change in the x -direction, the average distance

from a collision point to a y -axis across the CoM is labeled as $\bar{r}_{p_{y,x}}$. Similarly, one can use the subindex base to refer to the average collision distance of the base molecule $\bar{r}_{p_{base,i}}$ to any i axis across the CoM. One can then study the i -axis average distance variations relative to CoM changes in a coordinate direction j , with respect to the average value of the base molecule, i.e., $\bar{r}_{p_{i,j}}/\bar{r}_{p_{base,i}}$. A ratio larger than one, assuming no changes on the MoI, would ultimately result, as previously shown, in a shift toward lower mobility. A ratio smaller than one would suggest a shift toward higher mobility. Figures 6b–d and S9b–d plot $\bar{r}_{p_{i,j}}/\bar{r}_{p_{base,i}}$ ratios for the different j coordinate CoM artificial changes for iodoTMT and TMT, respectively (blue and orange dashed lines). Note that $\bar{r}_{p_{i,j}}/\bar{r}_{p_{base,i}} = 1$, so only two ratios appear in the figures. To see if the ratios are directly correlated with the expected mobility shifts, the numerical simulations appearing in Figure 4 are also shown in Figures 6 and S9 for comparison (red dashed lines).

As noted previously, the change in CoM also brings about a change on the MoI, which has its own separate effect. As such, if the observed effect of the mobility shifts would be due to changes in \bar{r}_p alone, one should expect the combination of ratios (orange and blue dashed lines in Figures 6 and S9) to behave in a similar fashion to the simulations. A major departure would suggest that the effects of the MoI dominate. While the actual CoM-related MoI mobility shifts are unknown, one can use instead the uniform spherical MoI mobility shifts from Figure 4 (MoI-only shift) as a reasonable approximation (green dashed lines in Figures 6 and S9). The expectancy is that if changes in \bar{r}_p are negligible, then positive and negative CoM changes will result in symmetrical evolutions toward lower mobilities closely resembling those of MoI-only changes. As can be observed in Figures 6b and S9b with CoM shifts in the $j = x$ -direction, the simulated shifts follow $\bar{r}_{p_{i,j}}/\bar{r}_{p_{base,i}}$ ratios rather than the MoI changes as it is expected that the \bar{r}_p effect is rather large (the x -direction corresponds in both cases to the elongated backbone of the ion). For the $j = y$ and $j = z$ -directions, the effects of the ratios are expected to be similar or smaller than the effect of the MoI-only changes, which is corroborated in Figures 6c,d and S9c,d and where the ratio trends are crudely followed. They are however sufficient to break the MoI-only symmetry, leaning toward the preferred ratio direction. Note that each i -based $\bar{r}_{p_{i,j}}/\bar{r}_{p_{base,i}}$ base ratio contributes independently, so the overall effect would be a weighted valuation. Given the geometries of our isotopomers, changes in the x -direction dominate over those in the other two directions. This can be observed in Figures 6c,d and S9c,d, where $\bar{r}_{p_{x,j}}$ ratios tend to influence the shift behavior more, i.e., blue dashed lines weigh more than their orange counterparts. This effect can also be isolated in eqs 2a, 2b, and 3, where the I_{ion}^- tensor multiplies $\vec{r}_p \times \vec{n}$. Upon a CoM change, which is not in the x -direction, the largest MoI changes in these ions are expected to occur in the I_{xx} -direction. A final discussion on how lower collision frequency may lead to lower mobilities can be reasoned through larger energy transfer upon collisions. A detailed description is provided in the Methods Section S5 of the SI.

CONCLUSIONS

The application of ultra-high-resolution ion mobility separation measurements to two sets of six isotopomers has revealed distinguishable mobility shifts, which cannot be accounted for by conventional ion mobility theory. IMoS 2 has provided numerical simulations that explicitly account for ion rotational effects while conserving linear and angular momentum. The simulations are in broad agreement with their experimental counterpart, being consistent with both the magnitude of the mobility shifts and the relative differences between isotopomers. The simulation study was expanded using strategically designed artificial isotopomers to explore how the changes in CoM and MoI affect the ion rotation, overall collision frequency, and energy transfer upon collisions, thus illuminating how structural details affect isotopomer mobility shifts.

Supplementary Material

Refer to Web version on PubMed Central for supplementary material.

ACKNOWLEDGMENTS

C.L. would like to acknowledge that this work is supported by the NSF Division of Chemistry under Grant No. 1904879 (Program officer Dr. Kelsey Cook). The efforts at PNNL were supported by the National Institute of General Medical Sciences (P41 GM103493–15 to R.D.S.), and measurements were performed in the Environmental Molecular Sciences Laboratory, a DOE OBER national scientific user facility at PNNL. C.P.H. also acknowledges partial support through the PNNL m/q Initiative-a Laboratory Directed Research and Development Program at PNNL. PNNL is a multiprogram national laboratory operated by Battelle for the DOE under contract DE-AC05–76RL01830.

REFERENCES

- (1). Chahrour O; Cobice D; Malone J J. *Pharm. Biomed. Anal* 2015, 113, 2–20. [PubMed: 25956803]
- (2). Lehmann WD *Mass Spectrom. Rev* 2017, 36, 58–85. [PubMed: 26919394]
- (3). Wojcik R; Nagy G; Attah IK; Webb IK; Garimella SVB; Weitz KK; Hollerbach A; Monroe ME; Ligare MR; Nielson FF; Norheim RV; Renslow RS; Metz TO; Ibrahim YM; Smith RD *Anal. Chem* 2019, 91, 11952–11962. [PubMed: 31450886]
- (4). Kaszycki JL; Bowman AP; Shvartsburg AA *J. Am. Soc. Mass Spectrom* 2016, 27, 795–799. [PubMed: 26944281]
- (5). Shvartsburg AA; Clemmer DE; Smith RD *Anal. Chem* 2010, 82, 8047–8051. [PubMed: 20815340]
- (6). Mason EA; McDaniel EW *Transport Properties of Ions in Gases*; John Wiley & Sons: New York, 1988.
- (7). Viehland LA; Mason E *Ann. Phys* 1975, 91, 499–533.
- (8). Larriba-Andaluz C; Prell JS *Int. Rev. Phys. Chem* 2020, 39, 569–623.
- (9). Valentine SJ; Clemmer DE *Anal. Chem* 2009, 81, 5876–5880. [PubMed: 19548697]
- (10). Kirk AT; Raddatz C-R; Zimmermann S *Anal. Chem* 2017, 89, 1509–1515. [PubMed: 28208278]
- (11). Viehland LA *Int. J. Ion Mobility Spectrom* 2016, 19, 11–14.
- (12). Schaefer C; Kirk AT; Allers M; Zimmermann S J. *Am. Soc. Mass Spectrom* 2020, 31, 2093–2101. [PubMed: 32875796]
- (13). Pathak P; Baird MA; Shvartsburg AA *J. Am. Soc. Mass. Spectrom* 2020, 31, 137–145. [PubMed: 32881519]
- (14). Pathak P; Baird MA; Shvartsburg AA *Anal. Chem* 2018, 90, 9410–9417. [PubMed: 29969234]
- (15). Mesleh MF; Hunter JM; Shvartsburg AA; Schatz GC; Jarrold MF *J. Phys. Chem. A* 1996, 100, 16082–16086.

- (16). Larriba-Andaluz C; Hogan CJ J. Chem. Phys 2014, 141, No. 194107. [PubMed: 25416874]
- (17). Uhlenbeck GE; De Boer J Studies in Statistical Mechanics; North-Holland, 1962.
- (18). Chouinard CD; Nagy G; Webb IK; Garimella SV; Baker ES; Ibrahim YM; Smith RD Anal. Chem 2018, 90, 11086–11091. [PubMed: 30102518]
- (19). Hollerbach AL; Conant CR; Nagy G; Monroe ME; Gupta K; Donor M; Giberson CM; Garimella SVB; Smith RD; Ibrahim YM J. Am. Soc. Mass. Spectrom 2021, 32, 996–1007. [PubMed: 33666432]
- (20). Larriba C; Hogan CJ Jr J. Comput. Phys 2013, 251, 344–363.
- (21). Wannier GH Bell Syst. Tech. J 1953, 32, 170–254.
- (22). Connolly ML J. Mol. Graphics 1993, 11, 139–141.

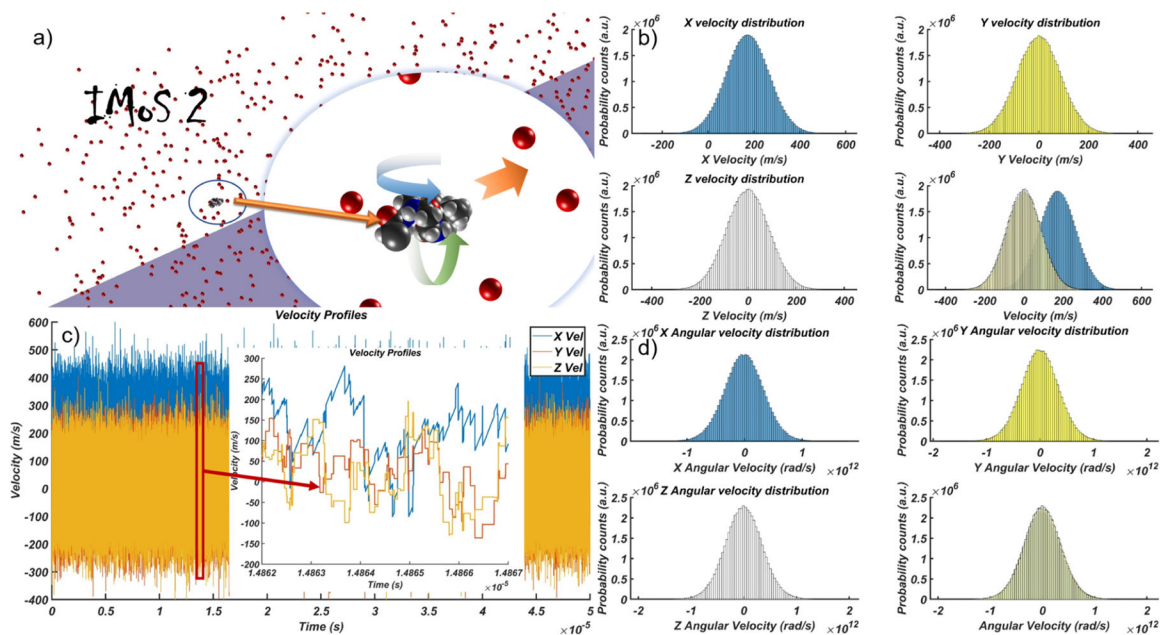


Figure 1.

Overview of IMoS 2 computational platform. (a) Mobility calculation using IMoS 2 embeds the ionic structure in a neutral gas subjected to an electric field. In the present work, the ion is considered rigid subjected to rotation and translation (see arrows). The single red molecules constitute the gas, while the ion corresponds to a DFT optimized structure. (b) Boltzmann velocity distributions in the X -, Y -, and Z -directions are obtained from the raw velocities. The fourth panel (lower right) represents the three distributions together to assist in checking for a nonsymmetric distribution in the X -direction (very slightly for the case here) (c) Raw result depicting velocities in X -, Y -, and Z -directions. The inset shows individual collisions (of all three velocities) as well as the effect acceleration in the X -direction (field direction). (d) Angular velocity distributions in the laboratory reference frame in X -, Y -, and Z -directions. The fourth panel (lower right) shows all three with no rotational preference evident.

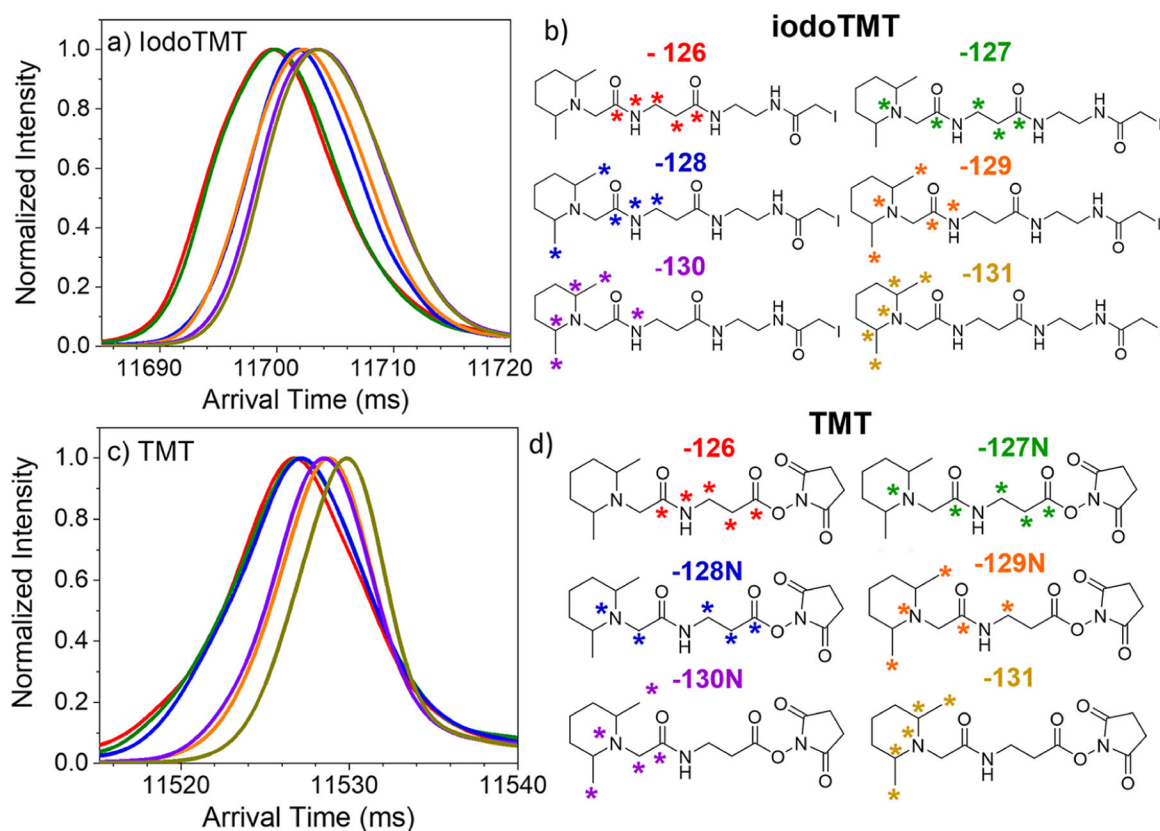


Figure 2.

Arrival time distributions of iodoTMT [(a); $452 + 5 + 1 = 458\ m/z$] and TMT [(c); $339 + 5 + 1 = 345\ m/z$] ion isotopomers, (a) and (c), respectively. (b) and (d), two-dimensional (2D) structures of iodoTMT and TMT isotopomers with heavy atom substitutions indicated by asterisks. Isotopomers only differ in the location of heavy atom substitution and produce mass resolved fragment ions upon collisional activation.

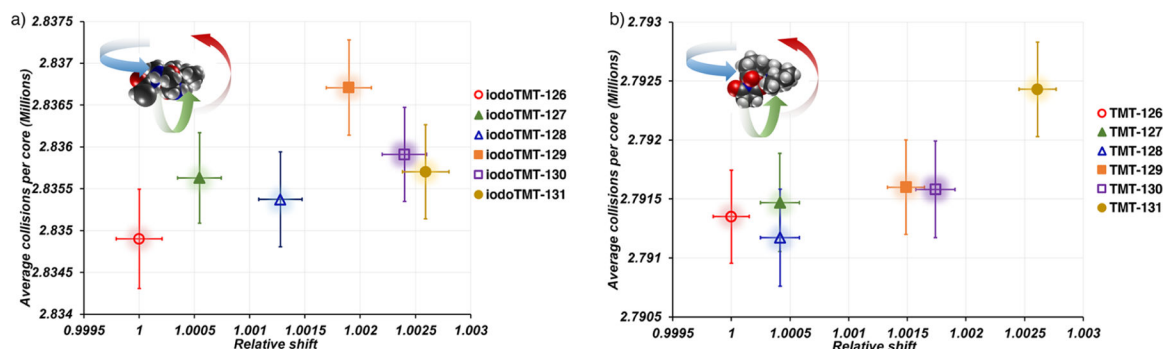


Figure 3.

Simulated relative arrival times after ~1.2 billion collisions (corresponding to ~65 ms) are shown for low energy structures of iodoTMT (a) and TMT (b) as a function of the average number of collisions per core (a total of 432 cores).

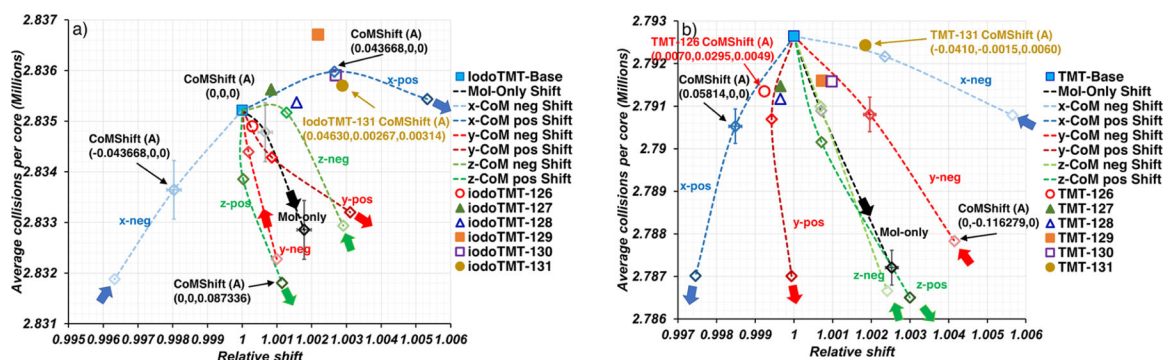


Figure 4.

Simulation mobility shifts due to CoM changes. Results show average collisions per core and relative mobility shifts with respect to a base molecule (blue square) for real and artificial isotopomers for (a) iodoTMT and (b) TMT molecular ions. The relative mobility shifts that result from only increasing the MoI (MoI-only shifts) relative to the base isotopomer are displayed using black diamonds. The relative mobility shifts from subsequent changes to the CoM and MoI by displacing 5 Da of mass from the CoM of the base isotopomer by either 4 or 8 Å in specified directions (xneg & xpos, yneg & ypos, zneg & zpos) are displayed with blue, red, and green diamonds, respectively. Dashed lines are used to connect the CoM and MoI-only shifts, using arrows as a guide from the largest negative to the largest positive CoM change. Given that the standard error is similar, it is only shown for some data to avoid overcrowding.

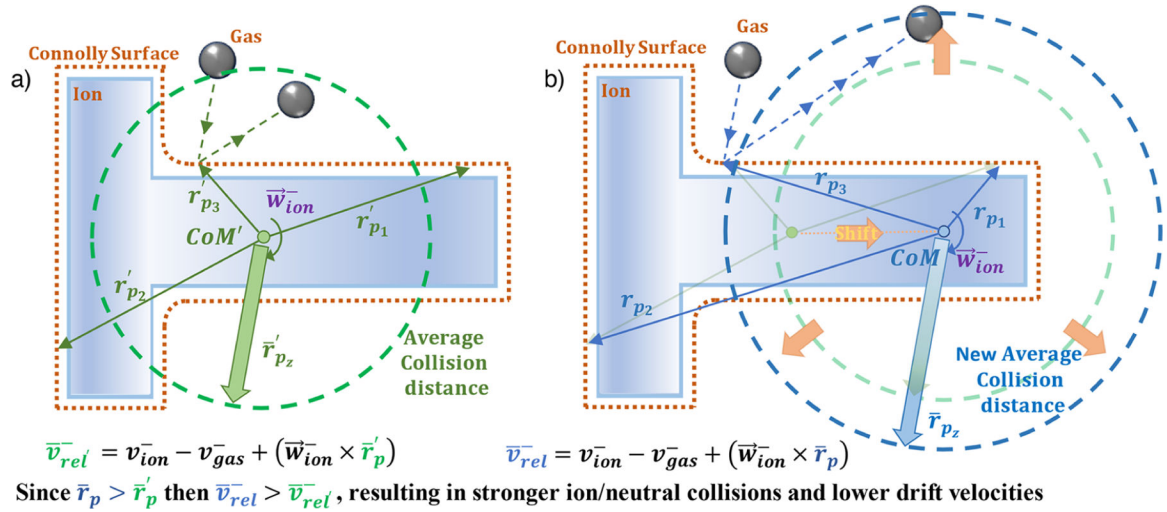


Figure 5.

Calculation of the average distance from CoM to collision surface (Connolly surface) for a 2D candidate structure for an initial CoM (a) and as the CoM is changed to a different location (b). \bar{v}_{ion} and \bar{w}_{ion} are the linear and angular velocities, and \bar{r}_p is the distance from the point of collision to the CoM of the ion.

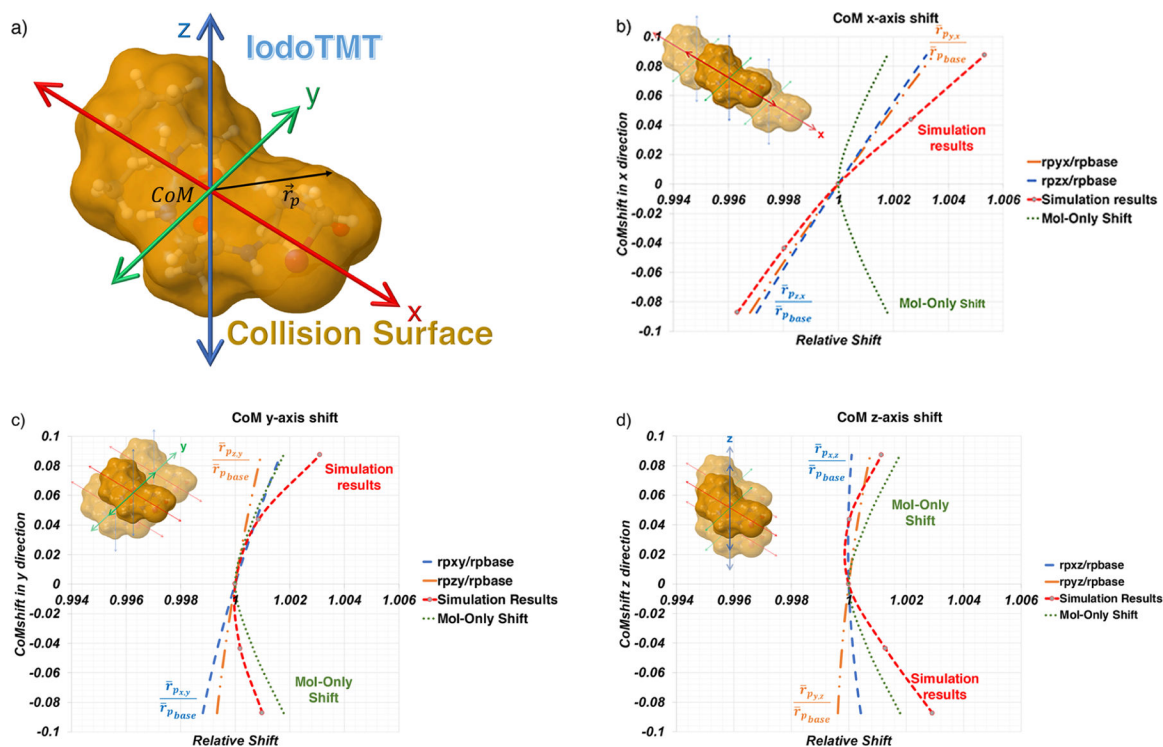


Figure 6.

(a) Molecular surface for iodoTMT molecule. (b–d) Relative mobility shifts as a function of the CoM shifts in the (b) x -, (c) y -, and (d) z -directions. Orange and blue dashed lines represent the ratio of average \vec{r}_p distance to the axis (i) between artificial isotopomers with CoM changes in the positive and negative j -directions, x (b), y (c), and z (d) to base molecule. The relative mobility shifts for the artificial isotopomers with Mol-only changes (green dashed line) and for the simulations of CoM changes in each j -direction (red dashed line) are also provided in (b–d) for reference.

Table 1.

Normalized ATD IMS Shifts from Experiments and Simulations for IodoTMT and TMT Isotopomers

isotopomer	experimental normalized shifts	simulated normalized shifts
IodoTMT-126	0 (reference)	0 ± 0.080
IodoTMT-127	0.06 ± 0.02	0.21 ± 0.076
IodoTMT-128	0.53 ± 0.04	0.49 ± 0.075
IodoTMT-129	0.66 ± 0.07	0.73 ± 0.078
IodoTMT-130	0.97 ± 0.03	0.93 ± 0.077
IodoTMT-131	1 (reference)	1 ± 0.080
TMT-126	0 (reference)	0 ± 0.058
TMT-127	0.05 ± 0.00	0.16 ± 0.064
TMT-128	0.13 ± 0.04	0.16 ± 0.064
TMT-129	0.67 ± 0.03	0.57 ± 0.060
TMT-130	0.50 ± 0.03	0.67 ± 0.064
TMT-131	1 (reference)	1 ± 0.060